Magnetic susceptibility of diluted magnetic semiconductors at low carrier densities

Adel Kassaian and Mona Berciu
Department of Physics and Astronomy, University of British Columbia, Vancouver, British Columbia, Canada V6T 1Z1
(Received 12 August 2004; revised manuscript received 11 November 2004; published 10 March 2005)

We calculate the static longitudinal and the transverse dynamic magnetic susceptibilities of (III,Mn)V diluted magnetic semiconductors, using the random phase approximation, for a simple impurity band model appropriate for the low charge carrier concentration regime. The magnetic susceptibilities are shown to depend sensitively on the amount of positional disorder of the Mn impurities. The results we obtain are consistent with previous studies of the spin wave spectrum and of the spatially inhomogeneous ferromagnetic state of these materials.

DOI: 10.1103/PhysRevB.71.125203 PACS number(s): 75.50.Pp, 75.40.Gb, 75.25.+z

I. INTRODUCTION

Diluted magnetic semiconductors (DMSs) are obtained by doping a semiconductor with magnetic impurities. To date, $Ga_{1-x}Mn_xAs$ has been the most studied[1] III-V DMS because it has the highest reliable critical temperatures recorded: 160 K for bulk samples[2] and 172 K in digitally doped heterostructures.[3] In $Ga_{1-x}Mn_xAs$, substitution of a fraction x of the Ga with Mn introduces both local Mn spins ($S=5/2$) and holes into the system. It is widely accepted that magnetization is due to charge-carrier mediated, effectively ferromagnetic (FM), interactions between the Mn spins.[1,4] It is known that these alloys are heavily compensated, with a hole concentration much smaller than the Mn concentration. DMSs are alloys, with inherent positional disorder of Mn atoms. Other types of defects, such as As antisites and Mn interstitials, are also present.[1,5] The spin-orbit coupling may play a significant role by making these interactions anisotropic,[6,7] although it is not clear to what extent.[8,9] A theoretical treatment which fully takes into account all these factors is not yet available. Instead, theoretical work tends to focus on different aspects of the problem.

Our recent work[10–15] has been focused on understanding the effects of *positional disorder* of the Mn impurities on the magnetic properties of these compounds. Disorder is known to induce localization of the states lying at the bottom of the band, below the mobility edge. When the Fermi energy crosses the mobility edge, the system undergoes a metal-insulator transition (MIT), at $x\sim 0.03$ in GaMnAs.[1] Since transport properties (metal versus insulator) are determined by the nature of the states near the Fermi energy (extended versus localized) one might argue that for the samples with the highest T_c, which are also the most metallic ones,[2] disorder effects are unimportant. However, the main applications of these materials are based on their magnetic properties. Unlike transport properties, the magnetic properties depend on the nature of *all* the occupied states, not only the ones near the Fermi energy, since *all* the charge carriers interact with the Mn spins. Disorder may thus influence magnetic properties considerably, certainly on the insulating side, but also above the MIT (even the most metallic GaMnAs samples have very short mean free paths).

In this work, we investigate the effects of positional disorder on the magnetic susceptibility of these materials. The model we study[10–14] is an impurity band model. It is expected to be (at least qualitatively) valid at low concentrations, below and near the MIT, where the disorder effects are likely to be largest and thus most easy to identify. Although we use GaMnAs as a prototype, other insulators, such as GaMnN and GeMn, may exhibit similar physics, if they are indeed DMSs.[16,17] In order to understand the effects of positional disorder, we contrast the behavior of ordered samples (where the Mn are assumed to be placed on an ordered cubic superlattice) with weakly, moderate, and fully disordered configurations, where we allow the randomness in the Mn positions to increase gradually.[10] It should be emphasized that the results for the ordered systems also apply to itinerant models,[18–20] provided that the appropriate mapping of parameters (discussed below) is performed. The method we employ is the random phase approximation (RPA); this, and the low density regime we consider distinguish our work from other recent computations of magnetic susceptibilities, based on Boltzmann equations.[21]

The paper is organized as follows: in Sec. II we briefly review the model and the self-consistent mean-field solution. In Sec. III we discuss the static longitudinal susceptibility. In Sec. IV we derive the generalized random phase approximation equations, which are used in Sec. V to compute the dynamical transverse susceptibility for ordered and disordered systems. Finally, Sec. VI contains our conclusions.

II. THE MODEL AND THE MEAN-FIELD APPROXIMATION

The model we investigate has been described in detail in Refs. 10–13. We briefly review it here. The host is assumed to have zinc-blende structure. N_d Mn dopants are placed at positions $\vec{R}_i$, $i=1,\ldots,N_d$ on an $N\times N\times N$ fcc sublattice, of lattice constant a (=5.65 Å for GaAs), corresponding to a doping $x=N_d/4N^3$. The number of charge carriers is fixed to $N_h=pN_d$, where $p<1$ due to compensation. We use periodic boundary conditions. The Hamiltonian we investigate is:

$$\mathcal{H}(t)=\sum_{i,j,\sigma} t_{ij}c^{\dagger}_{i\sigma}c_{j\sigma}+\sum_{i,j} J_{ij}\vec{S}_i\cdot\vec{s}_j-g\mu_B\sum_i \vec{B}(i,t)\cdot(\vec{s}_i+\vec{S}_i). \tag{1}$$

Here, $c^{\dagger}_{i\sigma}$ creates a charge carrier with spin σ in the impurity state centered at $\vec{R}_i$. The first term describes hopping of

charge carriers between impurity states, where $t_{ij}=2(1+r/a_B)\exp(-r/a_B)$ Ry, with $r=|\mathbf{R}_i-\mathbf{R}_j|$.[22] For Mn in GaAs, 1 Ry$\sim$110 meV and $a_B\approx 8$ Å.[10,23] This particular hopping Hamiltonian has been shown to describe an impurity band which has a mobility edge, as well as a characteristic energy for the occupied states in agreement with physical expectations (a detailed discussion of these issues is presented in the Appendix of Ref. 11, as well as Ref. 14). The second term describes the antiferromagnetic exchange between the Mn spin $\vec{S}_i$ and the charge carrier spin $\vec{s}_j=\frac{1}{2}c^\dagger_{j\alpha}\vec{\sigma}_{\alpha\beta}c_{j\beta}$ ($\vec{\sigma}$ are the Pauli spin matrices), which is proportional to the probability of overlap between the charge carrier trapped at $\vec{R}_j$ and the Mn spin at $\vec{R}_i$: $J_{ij}=J\exp(-2|\vec{R}_i-\vec{R}_j|/a_B)$. The exchange between a hole and its own Mn ($\vec{R}_i=\vec{R}_j$) is $J=15$ meV.[10,23] The third term describes the coupling to an external magnetic field. For simplicity, we assume that both types of spins have the same g-factor. The value of the holes' g is unimportant, because the magnetic properties are dominated by the Mn spins.[11]

This Hamiltonian obviously neglects several other possible terms. Since the system is heavily compensated, it must contain a significant amount of charged compensation centers. The electric potential created by these charged defects leads to the appearance of a disordered on-site energy, of type $\Sigma_{i\sigma}\epsilon_i c^\dagger_{i\sigma}c_{i\sigma}$. The spread in the distribution of ϵ_i is dependent on the amount of correlations between the positions of these charged defects, established during growth.[24] A Hubbard-like term $U\Sigma_i n_{i\uparrow}n_{i\downarrow}$ should be added to limit double-occupancy of the impurity states. Since the charge carrier density is low, one could argue that in fact longer range electron-electron repulsions are needed. We have studied the effect of adding such terms, as well as modeling differently the hopping term, in Ref. 11. They are found to lead to some quantitative changes, but no qualitatively new physics. As we propose to focus on the effects of positional disorder on the magnetic susceptibilities, we ignore such extra terms here. In Hamiltonian (1) we also assume that the impurity states have the simple s-wave symmetry typical of donor levels, ignoring the more complicated structure of impurity acceptor levels due to the multi-band valence band-structure.[23] Unless the spin-orbit coupling is very strong, we believe that this approximation also leads to only quantitative changes. The formalism we develop here can be straightforwardly generalized to take all these extra terms into account; however, we do not expect qualitative changes to the results we report.

We first consider a homogeneous, static external magnetic field, $\vec{B}(i,t)=B\vec{e}_z$. The mean-field solution, based on the customary factorization of the interaction term, was investigated in Refs. 10 and 11. We rederive it here using a variational approach. Then, we generalize this approach to spatial/time-dependent external fields, to find the RPA equations and dynamic response functions.

The idea is to replace the full interacting Hamiltonian,

$$\mathcal{H}^B=\sum_{i,j,\sigma}t_{ij}c^\dagger_{i\sigma}c_{j\sigma}+\sum_{i,j}J_{ij}\vec{S}_i\cdot\vec{s}_j-g\mu_B B\sum_i(s^z_i+S^z_i), \quad (2)$$

with the particular quadratic form[25]

$$\hat{\mathcal{K}}^B=\sum_{ij,\sigma}h^B_{ij,\sigma}c^\dagger_{i\sigma}c_{j\sigma}-\sum_i H^B_i S^z_i, \quad (3)$$

which minimizes the free energy[26] $\mathcal{F}(\hat{\mathcal{K}}^B)\geqslant\mathcal{F}_{eq}$, where

$$\mathcal{F}(\hat{\mathcal{K}}^B)=-k_BT\ln\mathcal{Z}^B_0+\mathrm{Tr}\{\hat{\mathcal{D}}^B_0[\hat{\mathcal{H}}^B-\hat{\mathcal{K}}^B]\}. \quad (4)$$

Here, $\hat{\mathcal{N}}=\Sigma_{i,\sigma}c^\dagger_{i\sigma}c_{i\sigma}$ is the particle number operator, $\hat{\mathcal{D}}^B_0=\exp[-\beta(\hat{\mathcal{K}}^B-\mu^B\hat{\mathcal{N}})]/\mathcal{Z}^B_0$ is the trial density matrix, where $\mathcal{Z}^B_0=\mathrm{Tr}\{\exp[-\beta(\hat{\mathcal{K}}^B-\mu^B\hat{\mathcal{N}})]\}$, and μ^B is the chemical potential. We use the upper index B to distinguish between solutions in different static external magnetic fields $B\vec{e}_z$. If $B=0$ we will drop this index.

We define the expectation values:

$$\rho^B_{ji,\sigma}=\mathrm{Tr}\{\hat{\mathcal{D}}^B_0c^\dagger_{i\sigma}c_{j\sigma}\}=-\frac{1}{\beta}\frac{\partial\ln\mathcal{Z}^B_0}{\partial h^B_{ij,\sigma}}, \quad (5)$$

$$\langle\vec{S}_i\rangle=\mathrm{Tr}\{\hat{\mathcal{D}}^B_0\vec{S}_i\}=S^B_{\mathrm{Mn}}(i)\hat{e}_z \quad (6)$$

where

$$S^B_{\mathrm{Mn}}(i)=\frac{1}{\beta}\frac{\partial\ln\mathcal{Z}^B_0}{\partial H^B_i}=B_S(\beta H^B_i). \quad (7)$$

and $B_S(x)=(S+\frac{1}{2})\coth[(S+\frac{1}{2})x]-\frac{1}{2}\coth(x/2)$ is the Brillouin function ($S=\frac{5}{2}$ for Mn). We then have:

$$\begin{aligned}\mathcal{F}(\hat{\mathcal{K}}^B)=&-k_BT\ln\mathcal{Z}^B_0+\sum_{ij,\sigma}t_{ij}\rho^B_{ji,\sigma}+\sum_{ij,\sigma}J_{ij}S^B_{\mathrm{Mn}}(i)\frac{\sigma}{2}\rho^B_{jj,\sigma}\\&-g\mu_BB\sum_i\left[S^B_{\mathrm{Mn}}(i)+\sum_\sigma\frac{\sigma}{2}\rho^B_{ii,\sigma}\right]-\sum_{ij,\sigma}h^B_{ij,\sigma}\rho^B_{ji,\sigma}\\&+\sum_i H^B_iS^B_{\mathrm{Mn}}(i).\end{aligned}$$

The variational parameters $h^B_{ij,\sigma}$ and H^B_i are obtained straightforwardly[26] from the minimization $\delta\mathcal{F}=0$:

$$H^B_i=g\mu_BB-\sum_{j,\sigma}\frac{\sigma}{2}J_{ij}\rho^B_{jj,\sigma}, \quad (8)$$

$$h^B_{ij,\sigma}=t_{ij}+\frac{\sigma}{2}\delta_{ij}\left[\sum_k J_{ik}S^B_{\mathrm{Mn}}(k)-g\mu_BB\right]. \quad (9)$$

These are the self-consistent mean-field equations. They can be written in the familiar form if the electronic part of the trial (or mean-field) Hamiltonian is diagonalized:

$$\mathcal{K}^B_{el}=\sum_{ij,\sigma}h^B_{ij,\sigma}c^\dagger_{i\sigma}c_{j\sigma}=\sum_{n\sigma}E^B_{n\sigma}a^\dagger_{n\sigma}a_{n\sigma} \quad (10)$$

through a unitary transformation:

$$a^\dagger_{n\sigma}=\sum_i\psi^B_{n\sigma}(i)c^\dagger_{i\sigma}. \quad (11)$$

The diagonalization condition is:

$$\sum_j h^B_{ij,\sigma}\psi^B_{n\sigma}(j)=E^B_{n\sigma}\psi^B_{n\sigma}(i). \quad (12)$$

These equations determine the self-consistent solution. We start with an initial guess for the values of $S^B_{\rm Mn}(i)$ (see Ref. 11 for details). We use Eqs. (9) and (12) to find the fermionic energies $E^B_{n\sigma}$ and wave functions $\psi^B_{n\sigma}(i)$. Using Eqs. (5), (10), and (11), the fermionic fields become:

$$\rho^B_{jj,\sigma} = \sum_n f(E^B_{n\sigma})|\psi^B_{n\sigma}(j)|^2, \tag{13}$$

where $f(E)=\{\exp[\beta(E-\mu^B)]+1\}^{-1}$ is the Fermi distribution and the chemical potential μ^B is given by:

$$\sum_{i,\sigma} \rho^B_{ii,\sigma} = \sum_{n,\sigma} f(E^B_{n\sigma}) = N_h. \tag{14}$$

Once the fermionic fields are known, using Eqs. (7) and (8) we can obtain the new spin expectation values $S^B_{\rm Mn}(i)$. We repeat the iterations until self-consistency is reached.

III. THE STATIC LONGITUDINAL SUSCEPTIBILITY

This response function characterizes the change in the total magnetization, when a static external magnetic field is applied parallel to the magnetization axis. We can separate it into two components, $\chi=\chi_{\rm Mn}+\chi_h$, where

$$\chi_{\rm Mn} = \frac{g\mu_B}{N_d}\sum_i \left.\frac{dS^B_{\rm Mn}(i)}{dB}\right|_{B=0}, \quad \chi_h = \frac{g\mu_B}{N_d}\sum_i \left.\frac{ds^B_h(i)}{dB}\right|_{B=0}.$$

(To obtain the susceptibility per unit volume, one needs to multiply by $n_{\rm Mn}=4x/a^3$). The charge carrier spin expectation values are [Eqs. (5) and (13)] $s^B_h(i)=\Sigma_\sigma \sigma \rho^B_{ii,\sigma}/2$.

One method to calculate these susceptibilities is by direct numerical evaluation of this derivative, e.g.,

$$\chi_{\rm Mn} \approx g\mu_B \left.\frac{S^B_{\rm Mn}-S_{\rm Mn}}{B}\right|_{g\mu_B B/J\ll 1}, \tag{15}$$

where $S^B_{\rm Mn}=\Sigma_i S^B_{\rm Mn}(i)/N_d$ and $S_{\rm Mn}=S^{B=0}_{\rm Mn}$ are the average Mn spin with and without a static magnetic field, which can be obtained directly from the mean-field solutions. The main issue with this approach is the proper choice of B and the proper self-consistency criterion to be used. Clearly, $S_{\rm Mn}$ and $S^B_{\rm Mn}$ must be computed to very high accuracy so that errors in the numerator of Eq. (15) are small relative to the small value of B chosen. We obtain good convergence with results of another method (described below) for $g\mu_B B=10^{-4}$ meV and self-consistency defined by the condition that the variation of the total magnetization in successive iterations is less than 10^{-6}. While reaching such high accuracy is time consuming, this method is the most efficient way to compute the static susceptibility for large system ($N_d>500$).

The more customary way to compute a linear response function, however, is to express it in terms of expectation values of the unperturbed system (i.e., $B=0$ quantities). Let us first derive the longitudinal susceptibility for an ordered system, i.e., one where the Mn impurities are assumed to be placed on a simple cubic superlattice inside the host semiconductor. In this case, due to invariance to translations, we have $S^B_{\rm Mn}(i)=S^B_{\rm Mn}$, $s^B_h(i)=s^B_h, \forall i$. The charge carrier part of the mean-field Hamiltonian [Eqs. (9) and (10)] has eigenfunctions which are plane-waves for all $\vec{k}$ inside the first Brillouin zone. We find:

$$E^B_{\vec{k}\sigma} = \epsilon_{\vec{k}} + \frac{\sigma}{2}(J_0 S^B_{\rm Mn} - g\mu_B B), \tag{16}$$

$$s^B_h = \frac{1}{2N_d}\sum_{\vec{k}\sigma} \sigma f(E^B_{\vec{k}\sigma}), \tag{17}$$

$$S^B_{\rm Mn} = B_S[\beta(g\mu_B B - J_0 s^B_h)]. \tag{18}$$

Here, $\epsilon_{\vec{k}}=\Sigma_{\vec{\delta}\neq 0} t_{\vec{\delta}} \exp(i\vec{k}\cdot\vec{\delta})$ is the kinetic energy of the noninteracting electrons, where $t_{\vec{\delta}}=t_{ij}$ for which $\vec{R}_i-\vec{R}_j=\vec{\delta}$. Also, $J_0=\Sigma_{\vec{\delta}} J_{\vec{\delta}}$, where $J_{\vec{\delta}}=J_{ij}$.

From Eq. (18), we find the spin contribution:

$$\frac{\chi_{\rm Mn}}{g\mu_B} = \beta\left(g\mu_B - J_0\frac{\chi_h}{g\mu_B}\right)B'_S(-\beta J_0 s_h), \tag{19}$$

where $B'_S(x)=(d/dx)B_S(x)$. From Eq. (17), we have:

$$\chi_h = \frac{g\mu_B}{2N_d}\sum_{\vec{k}\sigma} \sigma \left(\frac{dE^B_{\vec{k}\sigma}}{dB} - \frac{d\mu^B}{dB}\right)\Bigg|_{B=0} g(E_{\vec{k}\sigma}), \tag{20}$$

where $g(E)=(d/dE)f(E)$. From Eq. (16) we find:

$$\left.\frac{dE^B_{\vec{k}\sigma}}{dB}\right|_{B=0} = E^{(1)}_{\vec{k}\sigma} = \frac{\sigma}{2}\left(J_0\frac{\chi_{\rm Mn}}{g\mu_B} - g\mu_B\right). \tag{21}$$

Differentiating Eq. (14) with respect to B, we find:

$$\left.\frac{d\mu^B}{dB}\right|_{B=0} = \frac{\Sigma_{\vec{k}\sigma} E^{(1)}_{\vec{k}\sigma} g(E_{\vec{k}\sigma})}{\Sigma_{\vec{k}\sigma} g(E_{\vec{k}\sigma})}. \tag{22}$$

Substituting Eqs. (21) and (22) in Eq. (20) we get:

$$\chi_h = g\mu_B\gamma\left(g\mu_B - J_0\frac{\chi_{\rm Mn}}{g\mu_B}\right), \tag{23}$$

where

$$\gamma = \frac{1}{4N_d}\frac{[\Sigma_{\vec{k}\sigma}\sigma g(E_{\vec{k}\sigma})]^2 - [\Sigma_{\vec{k}\sigma} g(E_{\vec{k}\sigma})]^2}{\Sigma_{\vec{k}\sigma} g(E_{\vec{k}\sigma})}. \tag{24}$$

From Eqs. (23) and (19), we obtain the Mn susceptibility in the ordered case to be:

$$\chi_{\rm Mn} = \beta(g\mu_B)^2\frac{(1-J_0\gamma)B'_S(-\beta J_0 s_h)}{1-\beta J_0^2\gamma B'_S(-\beta J_0 s_h)} \tag{25}$$

while the hole susceptibility χ_h is:

$$\chi_h = (g\mu_B)^2\gamma\frac{1-J_0\beta B'_S(-\beta J_0 s_h)}{1-\beta J_0^2\gamma B'_S(-\beta J_0 s_h)}. \tag{26}$$

These static longitudinal susceptibilities are plotted as a function of temperature in Fig. 1. As expected, the critical temperature T_c is marked by a singularity. Since $s_h=0$ for $T\geqslant T_c$ and $B'_S(0)=S(S+1)/3$, the denominator in the susceptibilities gives:

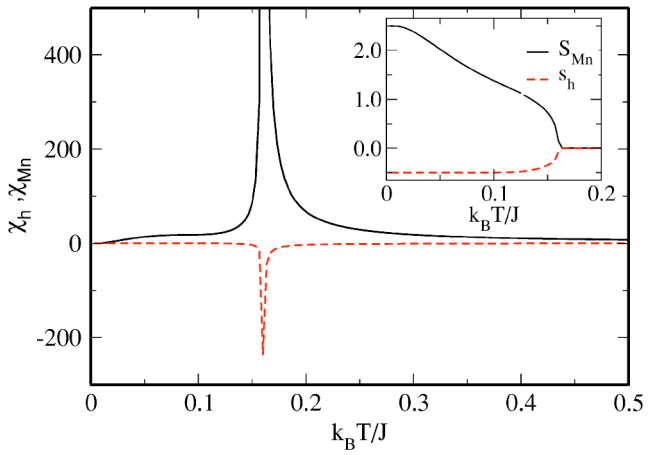

FIG. 1. $\chi_{\mathrm{Mn}}(T)$ (full) and $\chi_h(T)$ (dotted line), for an ordered Mn configuration with $N_d=512$, $x=0.00926$, and $p=10\%$. The inset shows the corresponding magnetizations.

$$k_BT_c = \gamma J_0^2 \frac{S(S+1)}{3}. \tag{27}$$

For $T \geqslant T_c$, $\Sigma_{\vec{k}\sigma}\sigma g(E_{\vec{k}\sigma})=0$ (spin degeneracy is restored). Then [Eq. (24)], $\gamma=-\Sigma_{\vec{k}\sigma}g(E_{\vec{k}\sigma})/4N_d=\int dE\Sigma_{\vec{k}\sigma}\delta(E-E_{\vec{k}\sigma})[-(d/dE)f(E)]/4N_d=\rho(E_F)/4n_{\mathrm{Mn}}$ (if $k_BT \ll E_F$), where $\rho(E_F)$ is the density of states per unit volume at the Fermi energy E_F. This value can also be obtained directly from Eq. (23), since in the absence of interactions ($J=0$), the hole susceptibility per unit volume $n_{\mathrm{Mn}}\gamma(g\mu_B)^2$ must equal the Pauli susceptibility.

In an effective mass approximation, $\epsilon_{\vec{k}}=\hbar^2k^2/2m^*$, $\rho(E_F) \sim m^*k_F \sim m^*(n_h)^{1/3} \rightarrow \gamma \sim m^*(px)^{1/3}/x$ (the factors contain only constants). Such an approximation can be used in two cases: (i) for itinerant models,[18–20] in which case $m^*=m_h$ is the mass of the heavy hole band, and $J_0 \rightarrow n_{\mathrm{Mn}}J_{pd}$ in order to obtain the same one-electron dispersion (see, e.g., Ref. 18). In this case, we regain the expected $T_c \sim x(px)^{1/3}$ mean-field scaling with the Mn and hole concentrations x and (px).[18–20] (ii) For an impurity model on an ordered lattice, for only nearest neighbor hopping t and $E_F \ll t$, we have $m^* \sim 1/(ta_L^2)$, where $a_L=a/x^{1/3}$ is the superlattice constant. It then follows that $T_c \sim p^{1/3}J_0^2/t$. Both J_0 and t depend on x through the distance between neighbors Mn. In Ref. 11 we showed numerically that at constant p, in the ordered impurity band case, $T_c \sim x$, so one can infer that here $T_c \sim xp^{1/3}$. In any event, disorder and thermal fluctuations considerably change these mean-field estimates.

Before discussing disordered systems, it is worth emphasizing why $\chi_h<0$. Each hole interacts antiferomagnetically with many Mn spins, each of which has its magnetization increased by the magnetic field. This favors an increased polarization of the holes, in a direction opposite to the applied field. Thus, the direct effect of the external field on the holes is more than offset by its indirect effect mediated through exchange with the Mn spins. As a result, in the paramagnetic phase χ_h is strongly enhanced from its noninteracting, T-independent Pauli value. From Eqs. (25) and (26), we see that

$$\frac{\chi_h}{\chi_{\mathrm{Pauli}}} = \frac{\chi_{\mathrm{Mn}}}{\beta(g\mu_B)^2} \frac{3-J_0\beta S(S+1)}{(1-J_0\gamma)S(S+1)}.$$

This increase can be formally assigned to an enhanced effective g-factor. Consistent with this phenomenology, huge Zeeman shifts have been measured in both II-VI and III-V DMSs.[27,28] Spintronic applications based on this high-T effect have been proposed recently.[29,30]

The longitudinal susceptibilities in the disordered case are calculated similarly. However, we now compute each contribution $\chi_{\mathrm{Mn}}(i)=dS^B_{\mathrm{Mn}}(i)/\,dB|_{B=0}$ and $\chi_h(i)=ds^B_h(i)/\,dB|_{B=0}$ [for simplicity, we set $g\mu_B=1$, i.e., measure the susceptibilities in units of $(g\mu_B)^2$]. This calculation is detailed in the Appendix. We end up with a system of linear equations for $\chi_{\mathrm{Mn}}(i)$ [Eq. (A8)]:

$$\sum_j [\delta_{ij}+R_{ij}]\chi_{\mathrm{Mn}}(j) = \beta(1-P_i)B_S'(\beta H_i)$$

The matrices $R \sim J^2$ and $P \sim J$ depend only on $B=0$ mean-field quantities [see the discussion following Eq. (A8)].

It is instructive to compare this result with the "conventional" statistical formula for static susceptibility:

$$\tilde{\chi}_{\mathrm{Mn}} = \frac{\beta}{N_d}\sum_{ij}[\langle \vec{S}_i\vec{S}_j\rangle - \langle \vec{S}_i\rangle\langle \vec{S}_j\rangle] \tag{28}$$

At the mean-field level $\langle \vec{S}_i\vec{S}_j\rangle=\langle \vec{S}_i\rangle\langle \vec{S}_j\rangle$ if $i \neq j$, since the mean-field density matrix $\mathcal{D}_0=\exp[-\beta(\mathcal{K}-\mu\mathcal{N})]$ is diagonal for different spins [see Eq. (3)]. It follows that $\tilde{\chi}_{\mathrm{Mn}}=\Sigma_i\tilde{\chi}_{\mathrm{Mn}}(i)/N_d$, where

$$\tilde{\chi}_{\mathrm{Mn}}(i) = \beta[\langle \vec{S}_i^2\rangle - \langle \vec{S}_i\rangle^2] = \beta B_S'(\beta H_i).$$

This is the solution one obtains if one sets the matrices R and P to zero, in the full system of linear equations shown above. Equivalently, comparison with Eq. (A1) shows that this "conventional" formula does not account for the contribution from the supplementary polarization of the holes. Since this is considerable (singular) near T_c, the "conventional" expression gives very wrong results for $T \sim T_c$, although it works well for $T \rightarrow 0$ or $T \gg T_c$, where the hole susceptibilities are very small. The reason for this failure is the fact that Eq. (28) holds when $\langle \ldots \rangle$ denotes the thermal average with the exact density matrix, not with the approximate mean-field density matrix. To be more precise, for a Hamiltonian such as of Eq. (1), the total susceptibility of the system is actually

$$\tilde{\chi} = \frac{\beta}{N_d}\sum_{ij}[\langle(\vec{S}_i+\vec{s}_i)\cdot(\vec{S}_j+\vec{s}_j)\rangle - \langle \vec{S}_i+\vec{s}_i\rangle\langle \vec{S}_j+\vec{s}_j\rangle]$$

where $\langle \ldots \rangle$ is the exact thermal average, which can be evaluated with Monte Carlo simulations. This susceptibility can be decomposed into a $\tilde{\chi}_{\mathrm{Mn}}$ and similar $\tilde{\chi}_h$ as in Eq. (28), but there is also a cross term containing terms like $\langle \vec{S}_i\vec{s}_j\rangle - \langle \vec{S}_i\rangle\langle \vec{s}_j\rangle$, which are not necessarily small near T_c. Ignoring these terms, i.e., approximating $\tilde{\chi} \approx \tilde{\chi}_{\mathrm{Mn}}$ in Monte Carlo simulations[12,31,33] is questionable, especially when $\tilde{\chi}$ is employed precisely to identify T_c.

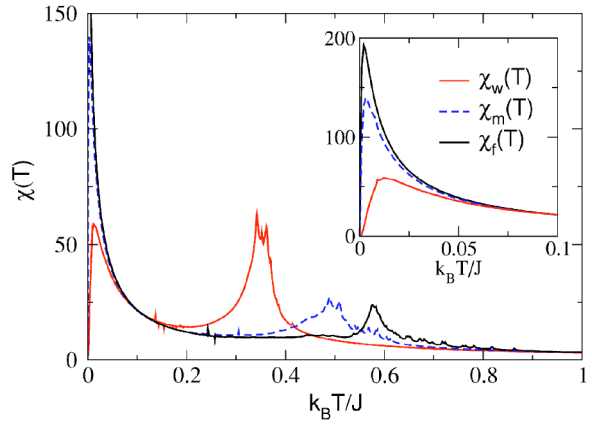

FIG. 2. Weak, medium and full disorder systems' susceptibilities vs T, for $N_d=216$, $x=0.00926$, and $p=10\%$. Inset focuses on the low-temperature region.

We analyze now the effect of disorder on the longitudinal susceptibility. We solve numerically the full system of coupled equations and find $\chi_{\mathrm{Mn}}\sim\Sigma_i\chi_{\mathrm{Mn}}(i)$. ($\chi_h$ can be found similarly. However, since $\chi_h\ll\chi_{\mathrm{Mn}}$, it follows that $\chi\approx\chi_{\mathrm{Mn}}$). The results shown in Fig. 2 are averaged over 30 disorder realizations. We denote by $\chi_w(T)$, $\chi_m(T)$, and $\chi_f(T)$ the susceptibilities of systems with weak, moderate and full disorder, as defined in Ref. 10. Unlike the ordered susceptibility which has only one peak at T_c (see Fig. 1), the susceptibility of disordered systems has two distinct peaks. One is at T_c, while the second peak appears at $T\ll T_c$ and is seen best in the inset. With increased disorder, this low-T peak has increased weight and amplitude and shifts to lower temperatures. It is due to the weakly coupled Mn spins which are positioned far from the regions of the sample where the holes are located with high probability.[11,15] These behave like free spins $\chi_{\mathrm{Mn}}(i)\sim 1/T$ except at extremely low temperatures $k_BT\sim H_i$, where they finally polarize [see Eqs. (7) and (8)]. The high-T peak in $\chi(T)$ marks the mean-field T_c. The high-T peak is determined by the behavior of the strongly coupled spins, from the regions where the holes are located.[11,15] As observed previously,[10–12] increased disorder leads to higher T_c. With increased disorder the high-T peak also broadens considerably. The explanation is provided below.

In Fig. 3 we show $\chi_{\mathrm{Mn}}(T)$ and $\chi_h(T)$ for a *single* disorder realization. Unlike the broad peak near T_c of the average χ_{Mn} shown in Fig. 2, here we see several narrow peaks in a range limited from below by the temperature where all holes become fully polarized. The highest-T peak occurs at the T_c of the individual sample. These narrow peaks appear symmetrically in both susceptibilities (however, $|\chi_h|\ll\chi_{\mathrm{Mn}}$). The number of such peaks and their positions are different for different samples. Less disordered samples have fewer peaks, in a smaller temperature range; the number of peaks increases with system size.[34] The origin of these peaks can be inferred from examining the values of $\chi_{\mathrm{Mn}}(i)$ at temperatures where peaks form. We find that each narrow peak is due to contributions from a distinct cluster of Mn spins, which are spatially close to one another and in a region where holes are found with large probability (these are strongly coupled spins). The magnetizations $S_{\mathrm{Mn}}(i)$ of spins from two different

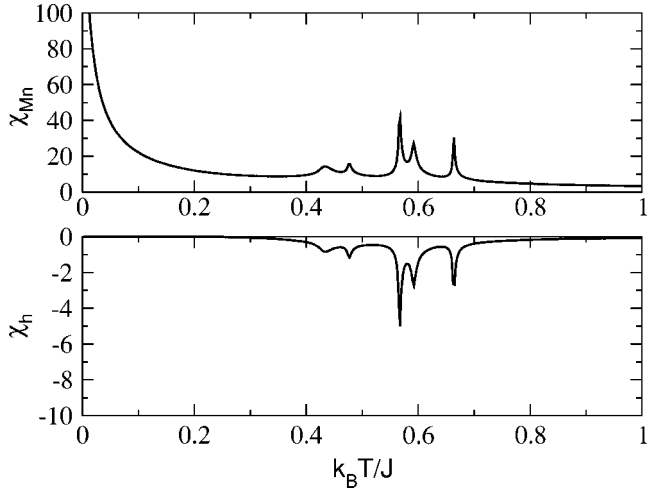

FIG. 3. $\chi_{\mathrm{Mn}}(T)$ and $\chi_h(T)$ for *single* fully disordered impurity configuration. $N_d=512$, $x=0.00924$, $p=0.10$.

clusters are shown in Fig. 4. Different clusters polarize at different "T_c," depending on their local environment. The local hole spin inside a cluster also becomes finite at the same T.[34] From Fig. 4 we see that these "local T_c" of individual clusters are the temperatures where χ has peaks, which thus signal the establishing of local FM correlations. The average over many disorder realizations results in a broad peak over the temperature range where these local FM correlations build up in the system. This range is larger for more disorder, which implies more inhomogeneity. On the other hand, it decreases with increasing x,[34] since for higher x fluctuations in the local concentration are reduced.

Strictly speaking, the true T_c of a sample is not related to this mean-field T_c estimate where various strongly coupled clusters begin to polarize. Instead, several magnetized clusters must appear all throughout the sample, and correlations between their magnetizations must be established (through exchange of polarized holes) before long-range magnetic order develops. This is qualitatively like the picture of magnetic polarons (each polarized cluster represents a magnetic polaron),[32] except that there T_c is marked by percolation of

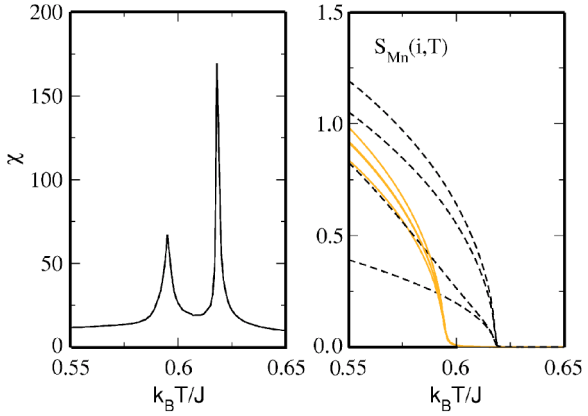

FIG. 4. Left: total susceptibility of a disordered sample, near T_c. Right: $S_{\mathrm{Mn}}(i,T)$ for spins belonging to two different clusters. $N_d=125$, $x=0.00924$, $p=0.10$.

the growing polarons, since the polarons cannot exchange polarized holes. This susceptibility peak at the mean-field T_c therefore denotes the characteristic temperature where the clusters (magnetic polarons, or local FM correlations) begin to form, also denoted by T^* in other studies.[33,35] Monte Carlo simulations are needed to determine T_c for the phase transition to long-range magnetic order.

IV. THE RANDOM-PHASE APPROXIMATION

We now consider the magnetic response to a general time-dependent magnetic field:

$$\vec{B}(i,t) = e^{\eta t}\int_{-\infty}^{\infty}\frac{d\omega}{2\pi}\frac{1}{V}\sum_{\vec{q}} e^{i(\vec{q}\cdot\vec{R}_i-\omega t)}\vec{B}(\vec{q},\omega) \tag{29}$$

turned on adiabatically at $t=-\infty$ ($\eta>0$ is infinitesimally small). The proper equations of motion for any operator $\mathcal{A}(t)$ and for the density matrix $\mathcal{D}(t)$ are obtained from the minimization of the action:[26]

$$S_{\mathcal{H}} = -\int_{t_i}^{t_f} dt\ \mathrm{Tr}\left\{\mathcal{A}\hbar\frac{d\mathcal{D}}{dt} + i\mathcal{A}[\mathcal{H},\mathcal{D}]\right\} + \mathrm{Tr}\,\mathcal{D}(t_f)\mathcal{A}(t_f),$$

subject to the constraints $\delta\mathcal{D}(t_i)=\delta\mathcal{A}(t_f)=0$. Here, $\mathcal{H}(t)$ is the full Hamiltonian of the system [Eq. (1) in this case]. Approximation schemes are obtained by solving $\delta S_{\mathcal{H}}=0$ for various classes of trial density matrices.

For a time-dependent mean-field calculation, the trial density matrix $\mathcal{D}(t)=e^{-\beta[\mathcal{K}(t)-\mu\mathcal{N}]}/\mathcal{Z}(t)$ is defined by a variational quadratic Hamiltonian $\mathcal{K}(t)$ and satisfies the initial condition $\mathcal{D}(-\infty)=\mathcal{D}_0$, where $\mathcal{D}_0$ is the mean-field density matrix of the unperturbed system. Like for the static mean-field derivation, we define the expectation values [compare with Eqs. (5) and (6)]:

$$\rho_{i\alpha,j\beta}(t) = \mathrm{Tr}\{\mathcal{D}(t)c_{j\beta}^{\dagger}c_{i\alpha}\}, \tag{30}$$

$$\vec{S}(i,t) = \mathrm{Tr}\{\mathcal{D}(t)\vec{S}_i\}. \tag{31}$$

$\mathcal{A}$ is taken to have a general quadratic dependence:

$$\mathcal{A}(t) = \sum_{\substack{i,j\\ \alpha\beta}} a_{i\alpha,j\beta}(t)c_{i\alpha}^{\dagger}c_{j\beta} - \sum_i \vec{A}_i(t)\cdot\vec{S}_i. \tag{32}$$

In terms of these quantities, $S_{\mathcal{H}}$ becomes:

$$\begin{aligned}S_{\mathcal{H}} = &-\hbar\int_{t_i}^{t_f} dt\left[\sum_{ij,\alpha\beta} a_{i\alpha,j\beta}(t)\frac{d\rho_{j\beta,i\alpha}(t)}{dt} - \sum_i \vec{A}_i(t)\cdot\frac{d\vec{S}(i,t)}{dt}\right]\\ &- i\int_{t_i}^{t_f} dt\sum_{i\alpha,j\beta,k\lambda} h_{i\alpha,j\beta}(t)[\rho_{j\beta,k\lambda}(t)a_{k\lambda,i\alpha}(t)\\ &- a_{j\beta,k\lambda}(t)\rho_{k\lambda,i\alpha}(t)] + \hbar\int_{t_i}^{t_f} dt\sum_i \vec{S}(i,t)\cdot[\vec{A}_i(t)\times\vec{H}_i(t)]\\ &+ \sum_{i\alpha,j\beta} a_{i\alpha,j\beta}(t_f)\rho_{j\beta,i\alpha}(t_f) - \sum_i \vec{A}_i(t_f)\cdot\vec{S}(i,t_f),\end{aligned}$$

where [compare with Eqs. (8) and (9)]

$$h_{i\alpha,j\beta}(t) = t_{ij}\delta_{\alpha\beta} + \delta_{ij}\frac{\vec{\sigma}_{\alpha\beta}}{2}\cdot\left[\sum_k J_{ik}\vec{S}(k,t) - g\mu_B\vec{B}(i,t)\right], \tag{33}$$

$$\vec{H}_i(t) = g\mu_B\vec{B}(i,t) - \sum_{j\alpha\beta} J_{ij}\frac{\vec{\sigma}_{\alpha\beta}}{2}\rho_{j\beta,j\alpha}(t). \tag{34}$$

From $\delta\mathcal{S}_{\mathcal{H}}/\delta a_{i\alpha,j\beta}=0$, where $\delta a_{i\alpha,j\beta}(t_f)=0$, we obtain the equation of motion for $\rho_{j\beta,i\alpha}(t)$:

$$i\hbar\frac{d\rho_{j\beta,i\alpha}(t)}{dt} = \sum_{k\lambda}[h_{j\beta,k\lambda}(t)\rho_{k\lambda,i\alpha}(t) - \rho_{j\beta,k\lambda}(t)h_{k\lambda,i\alpha}(t)], \tag{35}$$

which is just the matrix form of the expected $i\hbar d\rho/dt = [H,\rho]$. Similarly, the condition $\delta\mathcal{S}_{\mathcal{H}}/\delta\vec{A}_i(t)=0$, where $\delta\vec{A}_i(t_f)=0$, leads to the expected equation of motion:

$$\frac{d}{dt}\vec{S}(i,t) = -\vec{H}_i(t)\times\vec{S}(i,t). \tag{36}$$

Equations (35) and (36) describe the general time evolution for any value of the external field. We are interested in the linear regime of a perturbationally small external field. As a result, we need to solve Eqs. (35) and (36) to first order. We introduce the notation [see Eqs. (5) and (6)]:

$$\rho_{j\beta,i\alpha}(t) = \delta_{\alpha\beta}\rho_{ji,\alpha} + \delta\rho_{j\beta,i\alpha}(t) + \cdots,$$

$$\vec{S}(i,t) = \vec{e}_z S_{\mathrm{Mn}}(i) + \delta\vec{S}(i,t) + \cdots,$$

where we use the convention that all quantities denoted δX depend linearly on the external magnetic field $\vec{B}(i,t)$. To first order, the effective Hamiltonian (33) and the effective magnetic field (34) become [Eqs. (8) and (9)]:

$$h_{i\alpha,j\beta}(t) = \delta_{\alpha\beta}h_{ij,\alpha} + \delta_{ij}\delta h_{i,\alpha\beta}(t) + \cdots,$$

$$\vec{H}_i(t) = H_i\vec{e}_z + \delta\vec{H}_i(t) + \cdots,$$

where

$$\delta h_{i,\alpha\beta}(t) = \frac{\vec{\sigma}_{\alpha\beta}}{2}\cdot\left[\sum_k J_{ik}\delta\vec{S}(k,t) - g\mu_B\vec{B}(i,t)\right],$$

$$\delta\vec{H}_i(t) = g\mu_B\vec{B}(i,t) - \sum_{j\alpha\beta} J_{ij}\frac{\vec{\sigma}_{\alpha\beta}}{2}\delta\rho_{j\beta,j\alpha}(t). \tag{37}$$

We now substitute these expressions into Eqs. (35) and (36). The zero order (static) terms cancel out. After a time-domain Fourier transformation (taking into consideration the adiabatic term $e^{\eta t}$), we obtain

$$\begin{aligned}\hbar(\omega+i\eta)\delta\rho_{j\beta,i\alpha}(\omega) = &[\delta h_{j,\beta\alpha}(\omega)\rho_{ji,\alpha} - \delta h_{i,\beta\alpha}(\omega)\rho_{ji,\beta}]\\ &+ \sum_k[h_{jk,\beta}\delta\rho_{k\beta,i\alpha}(\omega) - h_{ki,\alpha}\delta\rho_{j\beta,k\alpha}(\omega)],\end{aligned} \tag{38}$$

$$i(\omega + i\eta)\delta\vec{S}(i,\omega) = \vec{e}_z \times [H_i \delta\vec{S}(i,\omega) - \delta\vec{H}_i(\omega) S_{\mathrm{Mn}}(i)]. \tag{39}$$

Let us consider first Eq. (39)—after all, we are interested in the linear change $\Sigma_i \delta\vec{S}(i,t)$ of the magnetization, related to the dynamic susceptibility. Equation (39) projects into two different equations for the components $\delta S_z(i,\omega)$ and $\delta S_+(i,\omega) = \delta S_x(i,\omega) + i\delta S_y(i,\omega)$:

$$(\omega + i\eta)\delta S_z(i,\omega) = 0,$$

$$(\omega - H_i + i\eta)\delta S_+(i,\omega) = -S_{\mathrm{Mn}}(i)\delta H_i^+(\omega). \tag{40}$$

The first equation shows that for $\omega \neq 0$, $\delta S_z(i,\omega) = 0$ and therefore $S_{\mathrm{Mn}}(i)$ is conserved (the static case $\omega = 0$ was investigated in the previous section). It follows that we can only define a transverse dynamical susceptibility. To calculate it, we need the values of $\delta H_i^+(\omega)$, which depend on $\delta\rho_{j\downarrow,j\uparrow}(\omega)$ [see Eq. (37)]. In turn, these depend on all $\delta\rho_{j\downarrow,k\uparrow}(\omega)$ components [see Eq. (38)]. Instead of working directly with these, it is more convenient to introduce

$$X_{nm}(\omega) = \sum_{ij} \psi^*_{m\downarrow}(j)\,\delta\rho_{j\downarrow,i\uparrow}(\omega)\psi_{n\uparrow}(i), \tag{41}$$

where $\psi_{n\sigma}(i)$ are the self-consistent mean-field eigenfunctions of Eq. (12) (here $B = 0$, since there is no static field applied) which are orthonormal and complete. Equations (40) and (38) (for $\beta = \downarrow, \alpha = \uparrow$) now become:

$$(\omega - H_i + i\eta)\delta S_+(i,\omega) = 2S_{\mathrm{Mn}}(i)\sum_{nm} J_{n\uparrow,m\downarrow}(i) X_{nm}(\omega) - g\mu_B S_{\mathrm{Mn}}(i) B_+(i,\omega), \tag{42}$$

$$(\hbar\omega + E_{n\uparrow} - E_{m\downarrow} + i\hbar\eta)X_{nm}(\omega) = [f(E_{n\uparrow}) - f(E_{m\downarrow})] \times \left[\sum_i J_{m\downarrow,n\uparrow}(i)\,\delta S_+(i\omega) - g\mu_B \sum_i \psi^*_{m\downarrow}(i)\psi_{n\uparrow}(i) B_+(i,\omega)\right], \tag{43}$$

where $J_{n\alpha,m\beta}(i) = \frac{1}{2}\Sigma_j J_{ij}\psi^*_{n\alpha}(j)\psi_{m\beta}(j)$, the eigenenergies $E_{n\sigma}$ and the occupation numbers $f(E_{n\sigma})$ depend on known static mean-field quantities. [Note: for $\omega \neq 0$, the chemical potential μ remains unchanged to its static self-consistent mean-field value, to first order, since from Eq. (38) it follows immediately that $(\hbar\omega + i\eta)\Sigma_{i,\alpha}\delta\rho_{i\alpha,i\alpha} = 0$].

The $N_d + N_d^2$ Eqs. (42) and (43) [or alternatively, Eqs. (38) and (39)] are the generalized random phase approximations (RPA) equations at finite temperature. In the limit $T = 0$, they indeed reduce to the RPA equations derived in Ref. 13. They can be replaced by a system of only N_d linear equations for $\delta S_+(i,\omega)$ by substituting the $X_{nm}(\omega)$ variables from (43) into (42). The final result is:

$$\sum_j M_{ij}(\omega)\,\delta S_+(j,\omega) = b_i(\omega), \tag{44}$$

where

$$M_{ij}(\omega) = \delta_{ij}(\omega - H_i + i\eta) - 2S_{\mathrm{Mn}}(i)\sum_{n,m} \frac{J_{n\uparrow,m\downarrow}(i)J_{m\downarrow,n\uparrow}(j)[f(E_{n\uparrow}) - f(E_{m\downarrow})]}{\hbar\omega + E_{n\uparrow} - E_{m\downarrow} + i\hbar\eta}, \tag{45}$$

$$b_i(\omega) = -g\mu_B S_{\mathrm{Mn}}(i)\left[B_+(i,\omega) + 2\sum_{n,m} J_{n\uparrow,m\downarrow}(i)\frac{f(E_{n\uparrow}) - f(E_{m\downarrow})}{\hbar\omega + E_{n\uparrow} - E_{m\downarrow} + i\hbar\eta} \times \sum_j \psi^*_{m\downarrow}(j)\psi_{n\uparrow}(j) B_+(j,\omega)\right]. \tag{46}$$

V. THE TRANSVERSE DYNAMICAL SUSCEPTIBILITY

The transverse dynamical susceptibility is defined as:

$$\delta S_+(\vec{q},\omega) = \frac{n_{\mathrm{Mn}}}{N_d}\sum_i e^{-i\vec{q}\cdot\vec{R}_i}\delta S_+(i,\omega) = \frac{\chi(\vec{q},\omega)}{g\mu_B} B_+(\vec{q},\omega) \tag{47}$$

for each transverse component of the applied field $B_+(i,\omega) = e^{i\vec{q}\cdot\vec{R}_i}B_+(\vec{q},\omega)/V$ [see Eq. (29)]. Note that all $b_i(\omega) \sim B_+(\vec{q},\omega)$ [Eq. (46)] and thus all $\delta S_+(i,\omega)$ of Eq. (44) are indeed proportional to $B_+(\vec{q},\omega)$. In other words, for each $\vec{q}$ and ω of interest, we can set $B_+(\vec{q},\omega) = 1 \rightarrow B_+(i,\omega) = e^{i\vec{q}\cdot\vec{R}_i}/V$. We can then compute the matrix elements $M_{ij}(\omega)$ and $b_i(\omega)$ for any finite temperature, and solve Eq. (44) for $\delta S_+(i,\omega)$. With this convention, the transverse susceptibility per unit volume is

$$\chi(\vec{q},\omega) = \frac{g\mu_B n_{\mathrm{Mn}}}{N_d}\sum\nolimits_i \exp(-i\vec{q}\cdot\vec{R}_i)\,\delta S_+(i,\omega).$$

In the ordered case, this calculation can be carried out explicitly using Eqs. (16)–(18). The result is:

$$\chi(\vec{q},\omega) = \frac{(g\mu_B)^2 n_{\mathrm{Mn}} S_{\mathrm{Mn}}[1 - J_{\vec{q}}F_{\vec{q}}(\omega)]}{\hbar\omega + J_0 s_h + \frac{1}{2}S_{\mathrm{Mn}}|J_{\vec{q}}|^2 F_{\vec{q}}(\omega)} \tag{48}$$

where $J_{\vec{q}} = \Sigma_{\vec{\delta}} e^{i\vec{q}\cdot\vec{\delta}} J_{\vec{\delta}}$ [$J_{\vec{\delta}} = J_{ij}$ for which $\vec{\delta} = \vec{R}_i - \vec{R}_j$]. $F_{\vec{q}}(\omega) = 1/N_d \Sigma_k [f(E_{\vec{k},\downarrow}) - f(E_{\vec{k}-\vec{q},\uparrow})]/[\hbar\omega + \epsilon_{\vec{k}-\vec{q}} - \epsilon_{\vec{k}} + J_0 S_{\mathrm{Mn}}]$ is the spin-polarized electron-hole "bubble" expected to appear in RPA-level approximations.

Singularities in $\chi(\vec{q},\omega)$ mark the spectrum $\hbar\omega_{\vec{q}}$ of the spin-wave modes. In Fig. 5, we plot $\chi(\vec{q},\omega)$ for different $\vec{q}$, at $T = 0$. The values $\hbar\omega_{\vec{q}}$ of the singularities indeed coincide with the spin-wave spectra of Ref. 13. At finite-T, $\chi(\vec{q},\omega)$ for the ordered system still has a single peak, but its energy first increases, then decreases with T. This behavior is generic, as shown in Fig. 6. Such non-monotonic behavior is easy to understand, since [see denominator of Eq. (48)] $\hbar\omega_{\vec{q}} = J_0|s_h| - \frac{1}{2}S_{\mathrm{Mn}}|J_{\vec{q}}|^2 F_{\vec{q}}(\omega_{\vec{q}})$. At low-$T$, $|s_h|$ is constant while S_{Mn} decreases with T (see inset of Fig. 1), and $\hbar\omega_{\vec{q}}$ increases. Once

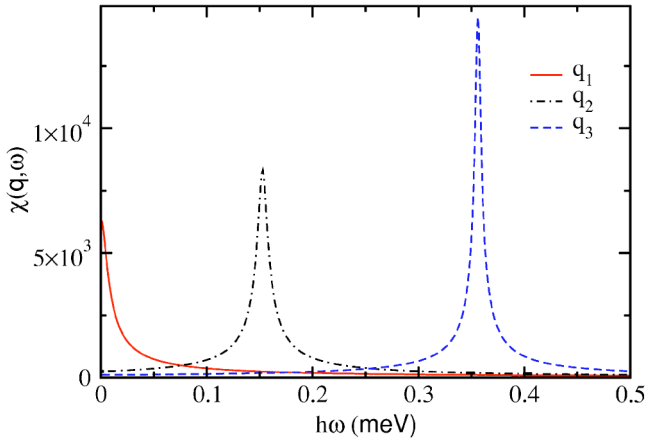

FIG. 5. $\chi(\vec{q},\omega)$ for the ordered case. $\vec{q}_1=0$, $\vec{q}_2=(\pi/15a)(2,0,0)$ and $\vec{q}_3=2\vec{q}_2$. $N_d=125$, $x=0.00924$, $p=0.1$, $T=0$.

the holes start to depolarize, $\hbar\omega_{\vec{q}}\to 0$. The exception is the case $\vec{q}=0$, where one finds $\chi(\vec{0},\omega)=(g\mu_B)^2 n_{\mathrm{Mn}} S_{\mathrm{Mn}}/(\hbar\omega)$. The $\omega=0$ singularity signals the Goldstone boson at all $T<T_c$ where one can define a transversal susceptibility.

In Fig. 7, we show $\chi(\vec{q},\omega)$ of a *single* fully disordered configuration, for four different values of $\vec{q}$. In contrast to the ordered case (Fig. 5), here we see multiple peaks in $\chi(\vec{q},\omega)$, which appear at the same energies for all values of $\vec{q}$. The explanation is that disorder breaks translational invariance and $\vec{q}$ is no longer a good quantum number. As discussed in Ref. 13, in this case many spin-wave modes become localized and even the extended modes do not carry well-defined momentum. As a result, an external magnetic field $B_+(\vec{q},\omega)$ can excite all the spin-waves of energy close to ω (conservation of energy) since conservation of momentum no longer holds. The narrow peaks in $\chi(\vec{q},\omega)$ for various $\vec{q}$ occur at the same frequencies because they couple to the same spin-wave modes. The differences are mostly in the amplitude of the peaks, but even these converge and $\chi(\vec{q},\omega)$ becomes roughly independent of $\vec{q}$ for moderate to large $\vec{q}$-values.

To restore invariance to translations, we have to average over all disorder realizations. The arguments presented above suggest that the averaged susceptibility is very different from

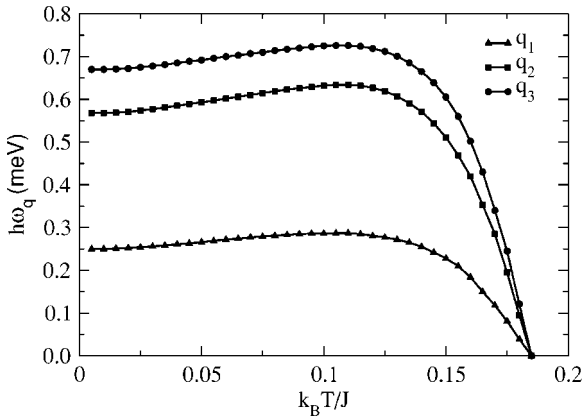

FIG. 6. Spin-wave energies $\hbar\omega_{\vec{q}}(T)$ for $\vec{q}_1=(\pi/9a)(1,1,0)$, $\vec{q}_2=2\vec{q}_1$, and $\vec{q}_3=3\vec{q}_1$; $N_d=216$, $x=0.00924$, $p=0.1$.

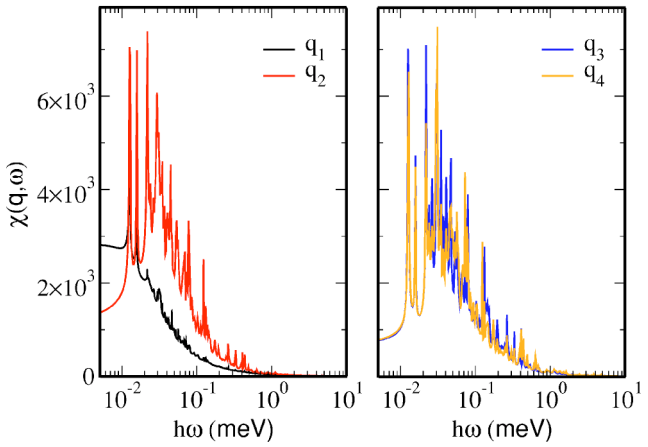

FIG. 7. $\chi(\vec{q},\omega)$ for an *individual* fully disordered configuration, for $\vec{q}_1=0$, $\vec{q}_2=(\pi/15a)(4,0,0)$, $\vec{q}_3=(\pi/15a)(8,0,0)$, and $\vec{q}_4=(\pi/15a)(8,8,8)$. $N_d=125$, $x=0.00924$ and $p=0.1$, $T=0$.

that of an ordered system even for weak disorder. This is indeed confirmed in Fig. 8, where we compare $\chi(\vec{q},\omega)$ for ordered and weakly disordered systems (averaged over 15 disorder configurations). Short wave vectors ($\vec{q}_1$) probe long length-scales, i.e., the extended modes. For weak disorder, these are not strongly perturbed and the results are fairly similar. However, at short wavelengths ($\vec{q}_2$, $\vec{q}_3$, and $\vec{q}_4$), the response in the disordered system is dominated by the localized modes and leads to a roughly $\vec{q}$-independent, extremely broad peak in the dynamic susceptibility. Note that even the extended modes, which occupy the center of the spectrum,[13] contain some short wavelength contributions and thus are probed by fields with large $\vec{q}$.

The change is even more drastic if disorder is increased and more modes become localized. A comparison for $\chi(\vec{q},\omega)$ for different levels of disorder, averaged over 20 disorder realizations, are shown in Fig. 9 on a logarithmic scale. The curves are not yet smooth, meaning that one needs to average over more samples. However, this is time consuming and the main features are already apparent. With increased disorder,

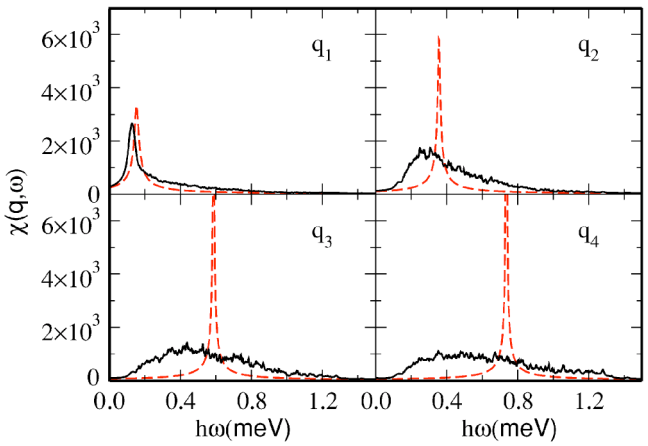

FIG. 8. $\chi(\vec{q},\omega)$ for ordered (dashed) and weakly disordered (full) systems. $T=0$, $x=0.00924$, $p=0.10$, $N_d=125$, and $\vec{q}_1=(\pi/15a)(2,0,0)$, $\vec{q}_2=2\vec{q}_1$, $\vec{q}_3=(\pi/15a)(4,4,0)$, $\vec{q}_4=(\pi/15a)(4,4,4)$.

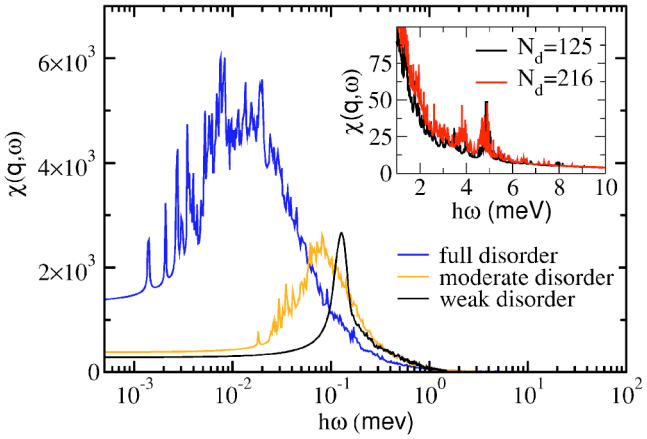

FIG. 9. $\chi(\vec{q},\omega)$ for ordered (dashed) and weakly disordered (full) systems, for $\vec{q}=(\pi/15a)(2,0,0)$, $T=0$, $x=0.00924$, $p=0.10$, $N_d=125$. Inset: the high-energy tail for fully disordered configurations, with $\vec{q}=(\pi/15a)(4,0,0)$ ($N_d=125$) and $\vec{q}=(\pi/18a)(4,0,0)$ ($N_d=125$).

the peaks become broader and shift toward lower energies. This is consistent with Ref. 13, which found an increased density of localized spin-waves at lower energies in the more disordered systems. Curves in Fig. 9 saturate to a finite value as $\omega\to 0$ because we used a finite value for η. From analyzing the dependence on η, we find[34] that $\chi(\vec{q},\omega)\sim 1/\omega$ as $\omega\to 0$ for all $\vec{q}$. This is the expected result: if one applies a static magnetic field transverse to the direction of the magnetization, the magnetization axis will rotate to become parallel to the applied field. This is a finite change in magnetization no matter how small the applied field is, and the static transverse susceptibility is infinite. In the ordered system, the momentum conservation prevents this singularity from being observed unless $\vec{q}=0$.

The high-energy tail of $\chi(\vec{q},\omega)$ is shown in the inset of Fig. 9, for two different system sizes. The $N_d=125/216$ curve has been been averaged over 40/20 disorder realizations. Because of the different system sizes, we have to investigate different vectors in the Brillouin zone. However, as already emphasized, here $\chi(\vec{q},\omega)$ is roughly independent of $\vec{q}$. Indeed, the two curves are very similar, suggesting also that finite-size effects are negligible. As discussed in Ref. 13, the high-energy collective modes are spin-waves localized inside strongly interacting clusters (magnetic polarons). In particular, the peak at $\sim$5 meV is due to clusters made of two nearest-neighbor Mn.[13]

On a technical note, we used $\eta=0.02/0.05J$ for ordered/disordered systems. A finite η implies a finite spin-wave lifetime, due to scattering on other spin-waves (neglected at the RPA level) and is necessary to avoid singularities in numerical computations. Also, all susceptibilities shown are in units of $(g\mu_B)^2 n_{\mathrm{Mn}}$.

VI. CONCLUSIONS

In previous work, we showed that positional disorder strongly influences the shape of the magnetization curve. Due to disorder, some of the charge carriers are localized in regions of the sample which have a large local Mn concentration. These regions (clusters or polarons) polarize at much higher temperatures than an ordered sample does, due to the much stronger effective coupling between the spins and holes. Charge carriers delocalized amongst several clusters help correlate their magnetizations at somewhat lower temperatures, thus leading to the appearance of long-range magnetic order. The concave magnetization curves we obtain[11] are in qualitative agreement with those obtained by other studies[36] which explicitly take into account the positional disorder, especially for low charge carrier densities. The large inhomogeneity induced by the localized states was also shown to influence the spin-wave spectrum, leading to localized modes at both low and high energies.[13] The low-energy localized spin-waves are, in fact, spin-flips of the weakly interacting spins, whereas the high-energy localized modes are spin-flips inside strongly coupled clusters.

Here, we show that the magnetic susceptibilities are also strongly sensitive to positional disorder. In particular, even very little disorder leads to a qualitatively different behavior of $\chi(\vec{q},\omega)$ compared to the ordered case, as shown in Fig. 8: instead of a Lorentzian centered at a well-defined spin-wave frequency $\hbar\omega_{\vec{q}}$, in the disordered case we obtain a very broad, roughly $\vec{q}$-independent peak, which extends over the entire range of the spin-wave spectrum. In the traditional weakly scattering case, the average over all disorder realizations leads to a finite lifetime of the excitations, but momentum is still a good quantum number. By contrast, here even small amounts of disorder induce localization of some of the charge-carriers,[11] which in turns leads to localization of some of the spin-wave modes.[13] Dealing with localization is well beyond the realm of applicability of weak-scattering arguments. Indeed, as we show here, the susceptibility in the presence of disorder is not just like that of an ordered system, but with a finite lifetime; instead, at any given $\vec{q}$ a transversal field can couple to all the spin-waves in the system, and therefore $\chi(\vec{q},\omega)$ is finite for all ω in the spin-wave spectrum. The only ingredient necessary for this dramatic change in the shape of $\chi(\vec{q},\omega)$ is the existence of some charge carrier localized states. On general grounds, one expects that to be the case at all x below and near the MIT. This prediction could be confirmed once neutron scattering experiments are performed on DMS.

The formalism we developed here can be trivially extended to more complicated cases, for instance to include anisotropies due to strain or spin-orbit coupling, noncollinear self-consistent ground-states or other supplementary terms such as on-site disorder, electron-electron interactions, etc. It is very unlikely that any such extra terms can completely inhibit the appearance of localization. As a result, their addition can only lead to some quantitative changes, but qualitatively the susceptibilities behave as the ones we derived using this simple impurity-band model.

ACKNOWLEDGMENTS

This work was supported by NSERC of Canada and by the Research Corporation.

APPENDIX: STATIC LONGITUDINAL SUSCEPTIBILITY

In this appendix we sketch the derivation of the static longitudinal susceptibility in the disordered case. Combining Eqs. (7) and (8), we find $S^B_{\rm Mn}(i)=B_S[\beta(B-\Sigma_j J_{ij}s^B_h(j))]$, (we set $g\mu_B=1$ for simplicity). Then,

$$\chi_{\rm Mn}(i)=\left.\frac{dS^B_{\rm Mn}(i)}{dB}\right|_{B=0}=\beta\left[1-\sum_j J_{ij}\chi_h(j)\right]B'_S(\beta H_i), \tag{A1}$$

where $B'_S(x)=d/dxB_S(x)$. Let us now compute $\chi_h(i)$. From Eq. (9) we find, to first order in B, that

$$h^B_{ij,\sigma}=h_{ij,\sigma}+\delta_{ij}\frac{\sigma}{2}\left[\sum_k J_{ik}\chi_{\rm Mn}(k)-1\right]B+\cdots \tag{A2}$$

and therefore [Eq. (10)] $\mathcal{K}^B_{el}=\mathcal{K}_{el}+B\mathcal{V}_{ex}+\cdots$, where

$$\mathcal{V}_{ex}=\sum_{i,\sigma}\frac{\sigma}{2}\left[\sum_j J_{ij}\chi_{\rm Mn}(j)-1\right]c^\dagger_{i\sigma}c_{i\sigma}.$$

We now use perturbation theory to find $E^B_{n\sigma}$ and $\psi^B_{n\sigma}(i)$ to first order in B. In a disordered system all degeneracies are lifted, and thus $E^B_{n\sigma}=E_{n\sigma}+E^{(1)}_{n\sigma}B+\cdots$, $\psi^B_{n\sigma}(i)=\psi_{n\sigma}(i)+\psi^{(1)}_{n\sigma}(i)B+\cdots$, where

$$E^{(1)}_{n\sigma}=\langle\psi_{n\sigma}|\mathcal{V}_{ex}|\psi_{n\sigma}\rangle=\sigma\sum_j J_{n\sigma,n\sigma}(j)\chi_{\rm Mn}(j)-\frac{\sigma}{2}, \tag{A3}$$

$$\begin{aligned}\psi^{(1)}_{n\sigma}(i)&=\sum_{m\neq n}\frac{\langle\psi_{m\sigma}|\mathcal{V}_{ex}|\psi_{n\sigma}\rangle}{E_{n\sigma}-E_{m\sigma}}\psi_{m\sigma}(i)\\&=\sigma\sum_{m\neq n,j}\frac{J_{m\sigma,n\sigma}(j)\chi_{\rm Mn}(j)}{E_{n\sigma}-E_{m\sigma}}\psi_{m\sigma}(i),\end{aligned} \tag{A4}$$

where $J_{n\alpha,m\beta}(i)=\frac{1}{2}\Sigma_j J_{ij}\psi^*_{n\alpha}(j)\psi_{m\beta}(j)$. Finally, differentiating Eq. (14), we find:

$$\left.\frac{d\mu^B}{dB}\right|_{B=0}=\frac{\Sigma_{n\sigma}E^{(1)}_{n\sigma}g(E_{n\sigma})}{\Sigma_{n\sigma}g(E_{n\sigma})}. \tag{A5}$$

Since $s^B_h(i)=\frac{1}{2}\Sigma_{n\sigma}\sigma|\psi^B_{n\sigma}(i)|^2f(E^B_{n\sigma})$, it follows that

$$\begin{aligned}\chi_h(i)=\sum_{n\sigma}\frac{\sigma}{2}\Bigg\{&[\psi^{(1)}_{n\sigma}(i)\psi^*_{n\sigma}(i)+\text{c.c.}]f(E_{n\sigma})\\&+|\psi_{n\sigma}(i)|^2\beta\left(E^{(1)}_{n\sigma}-\frac{d\mu}{dH}\right)g(E_{n\sigma})\Bigg\}.\end{aligned} \tag{A6}$$

Substituting the expressions for $E^{(1)}_{n\sigma}$, $\psi^{(1)}_{n\sigma}(i)$ and $(d\mu^B/dB)|_{B=0}$ from Eqs. (A3)–(A5), we obtain:

$$\chi_h(i)=\sum_j A_{ij}\chi_{\rm Mn}(j)+B_i, \tag{A7}$$

where

$$\begin{aligned}A_{ij}=\frac{1}{2}\sum_{n\sigma}\Bigg[&\sum_{m\neq n}f(E_{n\sigma})\frac{J_{m\sigma,n\sigma}(j)\psi^*_{n\sigma}(i)\psi_{m\sigma}(i)+\text{c.c.}}{E_{m\sigma}-E_{n\sigma}}\\&+\beta|\psi_{n\sigma}(i)|^2g(E_{n\sigma})\Bigg(J_{n\sigma,n\sigma}(j)\\&-\sigma\frac{\sum_{m\alpha}\alpha J_{m\alpha,m\alpha}(j)g(E_{m\alpha})}{\sum_{m\alpha}g(E_{m\alpha})}\Bigg)\Bigg]\end{aligned}$$

and

$$B_i=\frac{\beta}{4}\sum_{n\sigma}|\psi_{n\sigma}(i)|^2g(E_{n\sigma})\left[\sigma\frac{\sum_{m\alpha}\alpha g(E_{m\alpha})}{\sum_{m\alpha}g(E_{m\alpha})}-1\right].$$

Here it is worth mentioning that in Eq. (A7), the dominant term is $\Sigma_j A_{ij}\chi_{\rm Mn}(j)$ which is coming from the indirect effect of the external field on the Mn spins.

The set of Eqs. (A1) and (A7) relate $\chi_{\rm Mn}(i)$ and $\chi_h(i)$ to one another. The equations for determining $\chi_{\rm Mn}(i)$ at each site i are then:

$$\sum_j[\delta_{ij}+R_{ij}]\chi_{\rm Mn}(j)=\beta(1-P_i)B'_S(\beta H_i), \tag{A8}$$

where $R_{ij}=\beta B'_S(\beta H_i)\Sigma_k J_{ik}A_{kj}$ and $P_i=\Sigma_j J_{ij}B_j$. Once we know $\chi_{\rm Mn}(i)$, the values of $\chi_h(i)$ can be obtained from (A7). The total susceptibilities per unit volume are then $\chi_{\rm Mn}=n_{\rm Mn}(g\mu_B)^2\Sigma_i\chi_{\rm Mn}(i)/N_d$ and $\chi_h=n_{\rm Mn}(g\mu_B)^2\Sigma_i\chi_h(i)/N_d$.

[1] H. Ohno, J. Magn. Magn. Mater. **200**, 110 (1999).

[2] K. W. Edmonds, P. Bogusawski, K. Y. Wang, R. P. Campion, S. N. Novikov, N. R. S. Farley, B. L. Gallagher, C. T. Foxon, M. Sawicki, T. Dietl, M. Buongiorno Nardelli, and J. Bernholc, Phys. Rev. Lett. **92**, 037201 (2004).

[3] A. M. Nazmul, S. Sugahara, and M. Tanaka, Phys. Rev. B **67**, 241308(R) (2003).

[4] B. Beschoten, P. A. Crowell, I. Malajovich, D. D. Awschalom, F. Matsukura, A. Shen, and H. Ohno, Phys. Rev. Lett. **83**, 3073 (1999).

[5] K. M. Yu, W. Walukiewicz, T. Wojtowicz, I. Kuryliszyn, X. Liu, Y. Sasaki, and J. K. Furdyna, Phys. Rev. B **65**, 201303(R) (2002).

[6] G. Zaránd and B. Janko, Phys. Rev. Lett. **89**, 047201 (2002).

[7] G. A. Fiete, G. Zaránd, and K. Damle, Phys. Rev. Lett. **91**, 097202 (2003).

[8] L. Brey and G. Gomez-Santos, Phys. Rev. B **68**, 115206 (2003).
[9] C. Zhou, M. P. Kennett, X. Wan, M. Berciu, and R. N. Bhatt, Phys. Rev. B **69**, 144419 (2004).
[10] M. Berciu and R. N. Bhatt, Phys. Rev. Lett. **87**, 107203 (2000).
[11] M. Berciu and R. N. Bhatt, Phys. Rev. B **69**, 045202 (2004).
[12] M. P. Kennett, M. Berciu, and R. N. Bhatt, Phys. Rev. B **66**, 045207 (2002).
[13] M. Berciu and R. N. Bhatt, Phys. Rev. B **66**, 085207 (2002).
[14] M. Berciu and R. N. Bhatt, Phys. Rev. Lett. **90**, 029702 (2003).
[15] M. P. Kennett, M. Berciu, and R. N. Bhatt, Phys. Rev. B **65**, 115308 (2002).
[16] N. Theodoropoulos, A. F. Hebard, M. E. Overberg, C. R. Abernathy, S. J. Pearton, S. N. G. Chu, and R. G. Wilson, Appl. Phys. Lett. **78**, 3475 (2001).
[17] Y. D. Park, A. T. Hanbicki, S. C. Erwin, C. S. Hellberg, J. M. Sullivan, J. E. Mattson, T. F. Ambrose, A. Wilson, G. Spanos, and B. T. Jonker, Science **295**, 651 (2002).
[18] J. König, H.-H. Lin, and A. H. MacDonald, Phys. Rev. Lett. **84**, 5628 (2000); J. Schliemann, J. König, H.-H. Lin, and A. H. MacDonald, Appl. Phys. Lett. **78**, 1550 (2001).
[19] A. Chattopadhyay, S. Das Sarma, and A. J. Millis, Phys. Rev. Lett. **87**, 227202 (2001).
[20] T. Dietl, H. Ohno, and T. Matsukura, Phys. Rev. B **63**, 195205 (2001).
[21] C. Timm, F. von Oppen, and F. Höfling, Phys. Rev. B **69**, 115202 (2004); Y. Qi and S. Zhang, *ibid.* **67**, 052407 (2003).
[22] R. N. Bhatt, Phys. Rev. B **24**, 3630 (1981); **26**, 1082 (1982).
[23] A. K. Bhattacharjee and C. B. á la Guillaume, Solid State Commun. **113**, 17 (2000).
[24] C. Timm, F. Schfer, and F. von Oppen, Phys. Rev. Lett. **89**, 137201 (2002).
[25] The most general variational form would allow spin flips $\Sigma_{i,j,\sigma} h^B_{i\alpha,j\beta} c^\dagger_{i\alpha} c_{j\beta}$ and non-collinearity $\Sigma_i \vec{H}^B_i \cdot \vec{S}_i$ in $\hat{\mathcal{K}}$. However, a previous study of this model (Ref. 11) showed that the self-consistent mean-field ground state is always collinear, and thus the variational guess of Eq. (3) is appropriate.
[26] J.-P. Blaizot and G. Ripka, *Quantum Theory of Finite Systems* (MIT, Cambridge, MA, 1986).
[27] J. Furdyna, J. Appl. Phys. **64**, R29 (1988); S. Lee, M. Dobrowolska, J. K. Furdyna, and L. R. Ram-Mohan, Phys. Rev. B **61**, 2120 (2000).
[28] M. A. Zudov, J. Kono, Y. H. Matsuda, T. Ikaida, N. Miura, H. Munekata, G. D. Sanders, Y. Sun, and C. J. Stanton, Phys. Rev. B **66**, 161307(R) (2002).
[29] M. Berciu and B. Janko, Phys. Rev. Lett. **90**, 246804 (2003).
[30] M. Berciu, T. Rappoport, and B. Janko (unpublished).
[31] J. Schliemann, J. König and A. H. MacDonald, Phys. Rev. B **64**, 165201 (2001).
[32] A. Kaminski and S. Das Sarma, Phys. Rev. Lett. **88**, 247202 (2002); Phys. Rev. B **68**, 235210 (2003).
[33] M. Mayr, G. Alvarez, and E. Dagotto, Phys. Rev. B **65**, 241202 (2002).
[34] Adel Kassaian, M.Sc. thesis, University of British Columbia, 2004.
[35] G. Alvarez and E. Dagotto, Phys. Rev. B **68**, 045202 (2003).
[36] D. J. Priour, Jr., E. H. Hwang, and S. Das Sarma, Phys. Rev. Lett. **92**, 117201 (2004); S. Das Sarma, E. H. Hwang, and A. Kaminski, Phys. Rev. B **67**, 155201 (2003).